ISSN 2347 - 3983
Volume 7, No. 8 August 2019
International Journal of Emerging Trends in Engineering Research
Available Online at http://www.warse.org/IJETER/static/pdf/file/ijeter15782019.pdf
https://doi.org/10.30534/ijeter/2019/15782019

Grouping of COST 2100 Indoor Multipaths Using Simultaneous Clustering and Model Selection

Jojo F. Blanza[1], Lawrence Materum[2]
[1, 2] Department of Electronics and Communications Engineering, De La Salle University, Manila, Philippines, jojo_f_blanza@dlsu.edu.ph
[1]Electronics Engineering Department, University of Santo Tomas, Manila, Philippines, jfblanza@ust.edu.ph

ABSTRACT

Simultaneous Clustering and Model Selection (SCAMS) is introduced to cluster multipaths from COST 2100 channel model (C2CM). SCAMS determines not only the number of clusters but also the membership of the clusters. The study is the first to report clustering of multipaths that consider simultaneously the number of clusters and the membership of the clusters. Cluster identification and cardinality classification are dependent on the values of λ and γ, the parameters that weigh the penalty terms to avoid the trivial solution (all 1 matrix) of the affinity matrix. The clustered multipaths are compared with the reference multipaths that can be found in IEEE DataPort. The accuracy of the clustering approach is examined using the Jaccard index (η). The proposed clustering approach can achieve higher accuracy compared to popular multipath clustering approaches.

Keywords: channel models, clustering methods, multipath channels, radiowave propagation

1. INTRODUCTION

Channel modeling is important in studying the efficiency of wireless communications system. Channel modeling simulates the propagation channel prior to the implementation of a wireless communications network. Clustering approaches determine the characteristics of a channel model. For this reason, it is important to develop an accurate clustering approach to assess precisely the performance of a wireless communications system.

The European Cooperation in Science and Technology (COST) 2100 channel model can reproduce the properties of MIMO channels. C2CM have shown that multipath components with similar delay and angles are grouped into multipath clusters. A multipath component (MPC) is characterized in delay and angular domains by its delay, angle of departure (Azimuth of Departure (AoD), Elevation of Departure (EoD)), and angle of arrival (Azimuth of Arrival (AoA), Elevation of Arrival (EoA)). Multipaths generated by C2CM were applied to well-known clustering approaches in [1] to compare their accuracies using a single common C2CM dataset. The clustering approach in this study also uses the datasets generated by C2CM that are uploaded in IEEE DataPort [2] and detailed in [3]. This way, the accuracy of SCAMS [4] in clustering multipaths can be compared with the clustering approaches that also use C2CM datasets.

Clustering is the process of classifying data where objects that are similar are grouped (cluster) together. The field of application is wide but not limited to white blood cell classification [5] and wireless sensor networks [6]. On the other hand, the clustering approaches in [7]–[10] are applied to multipath clustering and consider only the number of clusters without taking into account the cardinality of the clusters. The problem with this clustering procedure is that it is possible that the number of clusters is correct but not the membership of the clusters. The study in [1] showed that the widely-used clustering approaches group multipaths at most half of the time. The result reveals that the clustering accuracy can still be improved. This study seeks to improve low clustering accuracy. Also, the study reports for the first time the clustering of multipaths by determining simultaneously the number of clusters and the membership of the clusters. The main contributions of this paper are (1) SCAMS is introduced to cluster multipaths and can be used as an alternative in channel modeling as it gives both the number of clusters and the membership of the clusters; and (2) the clustering approach shows potential due to improved accuracy compared to the results obtained in [1].

The paper is organized in the following way. Section 2 discusses the COST 2100 channel model. Section 3 describes the clustering approach. Section 4 shows the results of the clustering approach and compares with the reference multipaths. Section 5 concludes the work.

2. COST 2100 CHANNEL MODEL

A channel impulse response is a combination of MPCs from all the active multipath clusters. It is given as

$$h(t,\tau,\Omega^{\mathrm{BS}},\Omega^{\mathrm{MS}}) = \sum_{n\in\mathcal{C}} \sum_{p} \alpha_{n,p}\delta(\tau-\tau_{n,p})\delta(\Omega^{\mathrm{BS}}-\Omega^{\mathrm{BS}}_{n,p})\delta(\Omega^{\mathrm{MS}}-\Omega^{\mathrm{MS}}_{n,p}) \quad (1)$$

where $\mathcal{C}$ is the set of visible cluster indexes, $\alpha_{n,p}$ is the complex amplitude of the pth MPC in the nth cluster, $\Omega^{\mathrm{BS}}_{n,p}$ is the direction of departure (AoD, EoD), and $\Omega^{\mathrm{MS}}_{n,p}$ is the direction of arrival (AoA, EoA) of the MPC. C2CM is presented in [11] and discussed in detail in [12].

Generation of C2CM MPCs and multipath clusters is discussed in [3] and the datasets are uploaded in [2]. The two indoor scenarios are used as reference data in this study.

3. SIMULTANEOUS CLUSTERING AND MODEL SELECTION (SCAMS)

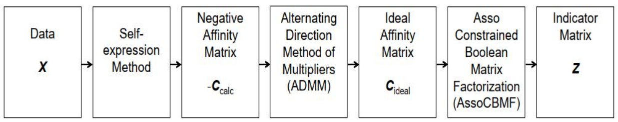

Figure 1: SCAMS Processing Steps

Algorithm 1: Alternating Direction Method of Multipliers

Input: Negative affinity matrix $\boldsymbol{W}$, parameters λ and γ
Initialize: $\boldsymbol{C}_{\text{ideal}} = \boldsymbol{H} = \boldsymbol{Y} = \boldsymbol{0}_{N\times N}$, $\mu = 10^6$, $\rho = 1.1$, $\mu_{\min} = 10^{-10}$ and $\varepsilon = 10^{-8}$.
while not converged **do**
Step 1 Fix the others and update $\boldsymbol{C}_{\text{ideal}}$ as
$\boldsymbol{C}_{\text{ideal}} = \operatorname{argmin}_{\boldsymbol{C}_{\text{ideal}}} \|\boldsymbol{C}_{\text{ideal}} - \boldsymbol{H} + \mu(\boldsymbol{W} + \boldsymbol{Y})\|_{\mathrm{F}}^2 + 2\mu\lambda \operatorname{rank}(\boldsymbol{C}_{\text{ideal}})$, s.t. $\boldsymbol{C}_{\text{ideal}} \in \mathbf{S}_+$.
Step 2 Fix the others and update $\boldsymbol{H}$ as
$\boldsymbol{H}' = \operatorname{argmin}_{\boldsymbol{H}} \|\boldsymbol{H} - \boldsymbol{C}_{\text{ideal}} - \mu\boldsymbol{Y}\|_{\mathrm{F}}^2 + 2\mu\gamma\|\boldsymbol{H}\|_0 + g(\boldsymbol{H})$,
$\boldsymbol{H} = \boldsymbol{H}' - \operatorname{diag}(\boldsymbol{H}') + \boldsymbol{I}$.
Step 3 Update the multipliers
$\mathbf{Y} = \mathbf{Y} + \frac{1}{\mu}(\boldsymbol{C}_{\text{ideal}} - \boldsymbol{H})$.
Step4 Update the parameter μ by
$\mu = \max\left(\frac{\mu}{\rho}, \mu_{\min}\right)$.
Step 5 Check the convergence conditions:
$\|\boldsymbol{C}_{\text{ideal}} - \boldsymbol{H}\|_\infty \le \varepsilon$.
endwhile

SCAMS, as illustrated in Figure 1, can solve both the problem on clustering and estimating the number of clusters. The clustering approach begins by formulating the affinity matrix $\boldsymbol{C}_{\text{calc}}$ using the self-expression method [13] where a given dataset $\boldsymbol{X}$ can be represented as $\boldsymbol{X}\boldsymbol{C}_{\text{calc}}$. The solution of (2) corresponds to $\boldsymbol{C}_{\text{calc}}$.

$$\min \|\boldsymbol{C}_{\text{calc}}\|_1 \quad \text{s.t. } \boldsymbol{X} = \boldsymbol{X}\boldsymbol{C}_{\text{calc}}, \quad \operatorname{diag}(\boldsymbol{C}_{\text{calc}}) = \boldsymbol{0} \tag{2}$$

By introducing an ideal affinity matrix $\boldsymbol{C}_{\text{ideal}}$ and denoting $\boldsymbol{W} = -\boldsymbol{C}_{\text{calc}}$, the clustering problem can be expressed as

$$\begin{aligned} &\min \quad \langle \boldsymbol{W}, \boldsymbol{C}_{\text{ideal}} \rangle, \\ &\text{s.t.} \quad \boldsymbol{z}_k\{0,1\}^M, \quad \textstyle\sum_{k=1}^{K} \boldsymbol{z}_k = \boldsymbol{e}_M, \\ &\boldsymbol{C}_{\text{ideal}} = \textstyle\sum_{k=1}^{K} \boldsymbol{z}_k \circ \boldsymbol{z}_k, \quad (\boldsymbol{C}_{\text{ideal}}) = K \end{aligned} \tag{3}$$

where $\langle\cdot,\cdot\rangle$ is the Frobenius inner product, $\boldsymbol{e}_M$ is an all one vector of size M while K is the number of clusters. (3) can be expressed as an augmented Lagrange function $\boldsymbol{\mathcal{L}}$

$$\begin{aligned} &\operatorname{tr}(\boldsymbol{W}^{\mathrm{T}}\boldsymbol{C}_{\text{ideal}}) + \lambda \operatorname{rank}(\boldsymbol{C}_{\text{ideal}}) + \gamma\|\boldsymbol{H}\|_0 + g(\boldsymbol{H}) \\ &\quad + \operatorname{tr}(\boldsymbol{Y}^{\mathrm{T}}(\boldsymbol{C}_{\text{ideal}} - \boldsymbol{H} + \operatorname{diag}(\boldsymbol{H}) - \boldsymbol{I})) \\ &+ \frac{1}{2\mu}\|\boldsymbol{C}_{\text{ideal}} - \boldsymbol{H} + \operatorname{diag}(\boldsymbol{H}) - \boldsymbol{I}\|_{\mathrm{F}}^2, \quad \text{s.t. } \boldsymbol{C}_{\text{ideal}} \in \boldsymbol{S}_+ \end{aligned} \tag{4}$$

where g is the indicator function of the convex set $[0,1]^{\mathrm{M}\times\mathrm{M}}$, which returns 0 if it is in the set, ∞ otherwise, $\boldsymbol{H}$ is an intermediate variable introduced to make the problem tractable, $\boldsymbol{Y}$ is the Lagrange parameter, $\mu > 0$ is a penalty parameter, $\|\cdot\|_0$ is the ℓ_0 norm which counts the number of nonzero elements, λ and γ are the parameters to weigh the respective penalty terms, and $\mathbf{S}_+$ is the positive semi-definite cone. The function can be minimized with respect to $\boldsymbol{C}_{\text{ideal}}$ and $\boldsymbol{H}$ alternatingly, by fixing the other variable, and then updating $\boldsymbol{Y}$. Algorithm 1 shows the overall framework of the Alternating Direction Method of Multipliers (ADMM) [14] and is used to solve for $\boldsymbol{C}_{\text{ideal}}$ which can be factorized as $\boldsymbol{Z}\boldsymbol{Z}^{\mathrm{T}}$ where $\boldsymbol{Z}$ is an indicator matrix whose rows indicate to which cluster a point belongs. $\boldsymbol{Z}$ can be solved by the AssoConstrained Boolean Matrix Factorization (AssoCBMF)

Algorithm 2: AssoConstrained Boolean Matrix Factorization

Input: $\boldsymbol{C}_{\text{ideal}}, K_0$
Initialize: Construct the Boolean matrix ${\boldsymbol{C}_{\text{ideal}}}^{\boldsymbol{B}}$ from $\boldsymbol{C}_{\text{ideal}}$ with rounding threshold $t_{\boldsymbol{B}} = 0.5$, $\boldsymbol{Z}^{\boldsymbol{B}} \leftarrow [\ \ ]$, $e = \infty$, $r_{\text{thresh}} = 0.1$.
for $\nu = 0.1, 0.2, \ldots, 1$ **do**
Construct $\boldsymbol{D}^{\boldsymbol{B}}$ with
$\boldsymbol{D}^{\boldsymbol{B}}(i,j) = \dfrac{\langle {\boldsymbol{C}_{\text{ideal}}}^{\boldsymbol{B}}(i,:), {\boldsymbol{C}_{\text{ideal}}}^{\boldsymbol{B}}(j,:)\rangle}{\langle {\boldsymbol{C}_{\text{ideal}}}^{\boldsymbol{B}}(j,:), {\boldsymbol{C}_{\text{ideal}}}^{\boldsymbol{B}}(j,:)\rangle} > \nu$.
for $k = 1, 2, \ldots, K_0$ **do**
$i = \operatorname{argmin}_i \left|{\boldsymbol{C}_{\text{ideal}}}^{\boldsymbol{B}} \oplus ([\boldsymbol{Z}^{\boldsymbol{B}}\boldsymbol{D}^{\boldsymbol{B}}(:,i)] \circ [\boldsymbol{Z}^{\boldsymbol{B}}\boldsymbol{D}^{\boldsymbol{B}}(:,i)]^{\mathrm{T}})\right|$.
$\boldsymbol{Z}^{\boldsymbol{B}} \leftarrow [\boldsymbol{Z}^{\boldsymbol{B}}\boldsymbol{D}^{\boldsymbol{B}}(:,i)]$.
Delete all j − th columns with
$\dfrac{\langle \boldsymbol{D}^{\boldsymbol{B}}(:,i), \boldsymbol{D}^{\boldsymbol{B}}(:,j)\rangle}{\|\boldsymbol{D}^{\boldsymbol{B}}(:,i)\|\|\boldsymbol{D}^{\boldsymbol{B}}(:,j)\|} > r_{\text{thresh}}$ from $\boldsymbol{D}^{\boldsymbol{B}}$
if $\boldsymbol{D}^{\boldsymbol{B}}$ is empty **or** min. $\left|{\boldsymbol{C}_{\text{ideal}}}^{\boldsymbol{B}} \oplus \left(\boldsymbol{Z}^{\boldsymbol{B}} \circ \boldsymbol{Z}^{\boldsymbol{B}^{\mathrm{T}}}\right)\right|$,
s.t. $\boldsymbol{Z}^{\boldsymbol{B}^{\mathrm{T}}} \circ \boldsymbol{Z}^{\boldsymbol{B}} = \boldsymbol{I}_{K\times K}$ is not reduced in this loop
break
end if
if $\left\|\boldsymbol{C}_{\text{ideal}} - \boldsymbol{Z}^{\boldsymbol{B}}\boldsymbol{Z}^{\boldsymbol{B}^{\mathrm{T}}}\right\|_{\mathrm{F}}^2 < e$
$\boldsymbol{Z}^{\boldsymbol{B}^*} = \boldsymbol{Z}^{\boldsymbol{B}}$.
$e = \left\|\boldsymbol{C}_{\text{ideal}} - \boldsymbol{Z}^{\boldsymbol{B}}\boldsymbol{Z}^{\boldsymbol{B}^{\mathrm{T}}}\right\|_{\mathrm{F}}^2$.
end if
end for
end for
return $\boldsymbol{Z}^{\boldsymbol{B}^*}$

shown in Algorithm 2 where superscript $\boldsymbol{B}$ is a "Boolean" matrix containing only 0's and 1's, $|\cdot|$ is the norm of a Boolean matrix and defined as the number of 1's in it, $\oplus$ is the Exclusive-OR operation applied element-wise and defined as the normal addition but with $1 + 1 = 0$, $\boldsymbol{D}(i,j)$ is the association accuracy for rule $\boldsymbol{C}_{\text{ideal}}{}^{\boldsymbol{B}}(j,:) \Rightarrow G^{\boldsymbol{B}}(i,:)$, and r_{thresh} is a threshold. The AssoCBMF algorithm [4] gives the number of clusters and the membership of the clusters.

4. RESULTS

The datasets in [2] which are used as reference data in

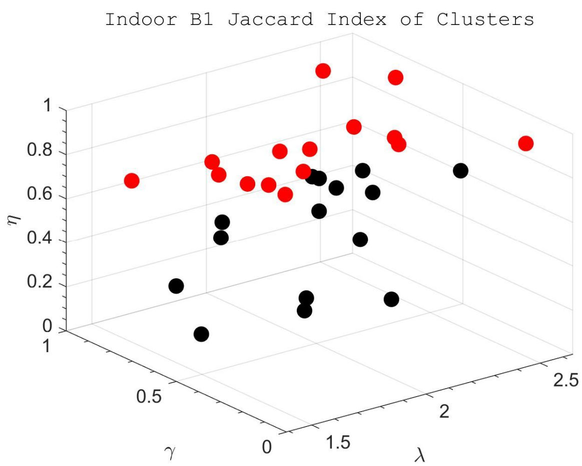

(a) Jaccard index of clusters with mean of 0.6034

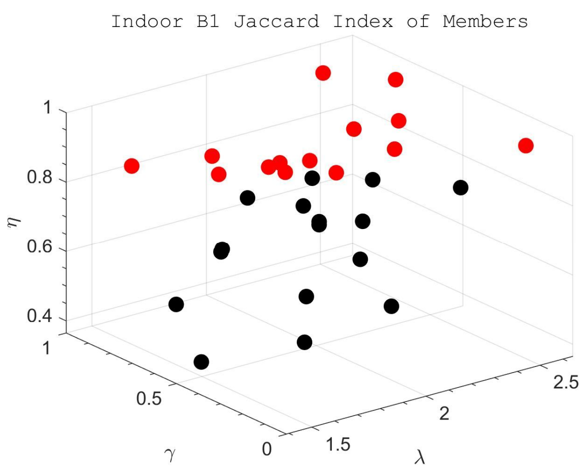

(b) Jaccard index of members with mean of 0.7305

Figure 2: Jaccard index as a function of λ and γ of Indoor B1 where red colors are indices higher than the mean

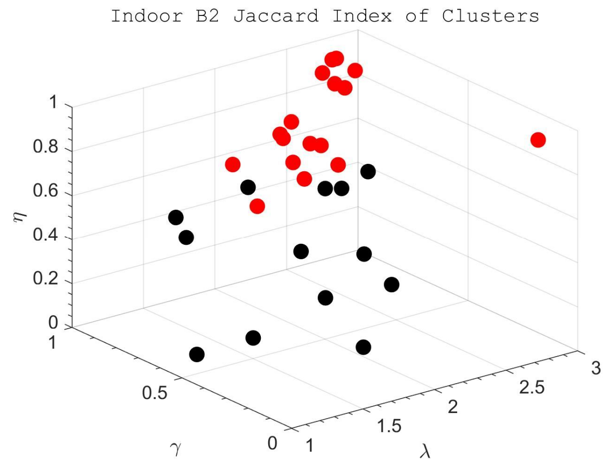

(a) Jaccard index of clusters with mean of 0.6487

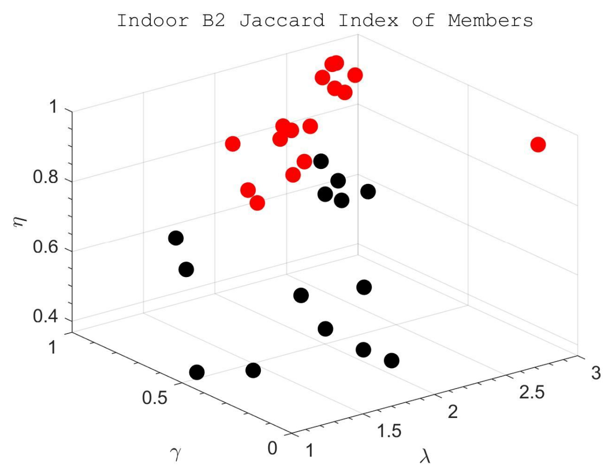

(b) Jaccard index of members with mean of 0.7352

Figure 3: Jaccard index as a function of λ and γ of Indoor B2 where red colors are indices higher than the mean

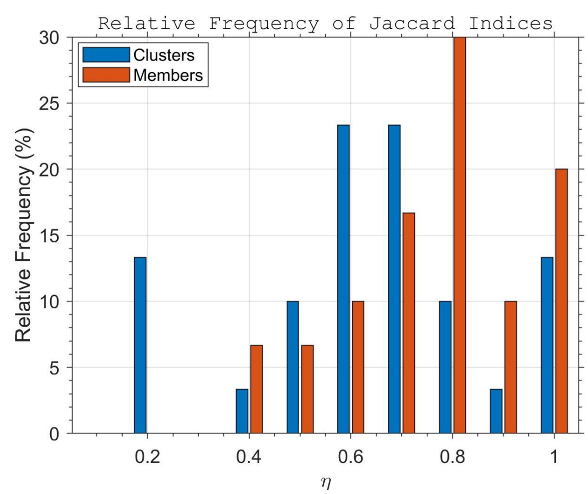

Figure 4: Relative frequency of Jaccard indices for Indoor B1

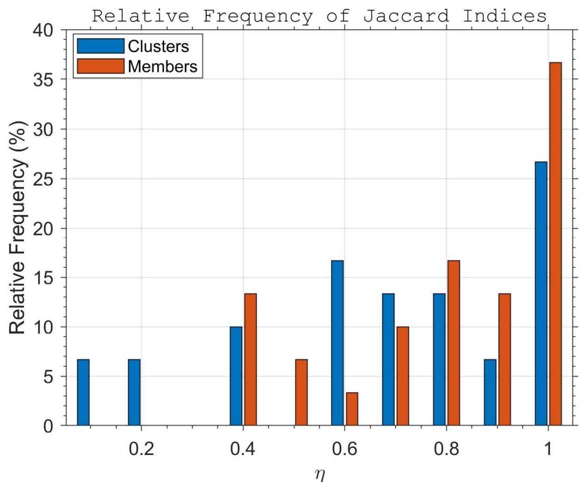

Figure 5: Relative frequency of Jaccard indices for Indoor B2

There are thirty datasets for each channel scenario with a different number of multipaths and different clusters. The whitened data of columns 1 to 7 in [2] are normalized [0,1] using

$$X_{\text{normalized}} = \frac{(X_{\text{whitened}} - X_{\min})}{(X_{\max} - X_{\min})} \tag{5}$$

where $X_{\text{normalized}}$ is the normalized value of the whitened data, X_{whitened} is the whitened data in columns 1 to 7, $X_{\max}$ is the maximum data of each column, and $X_{\min}$ is the minimum data of each column. The data are normalized to make sure that the affinities are positive values [0,1] which greatly affect the clustering results. Jaccard index (η) is used to compare the similarity between the computed data and the reference data. The similarity measure is defined as

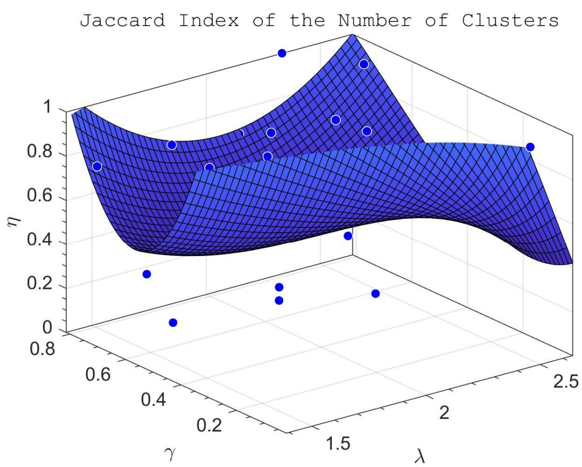

Figure 6: Jaccard index of the number of clusters vs λ and γ for Indoor B1

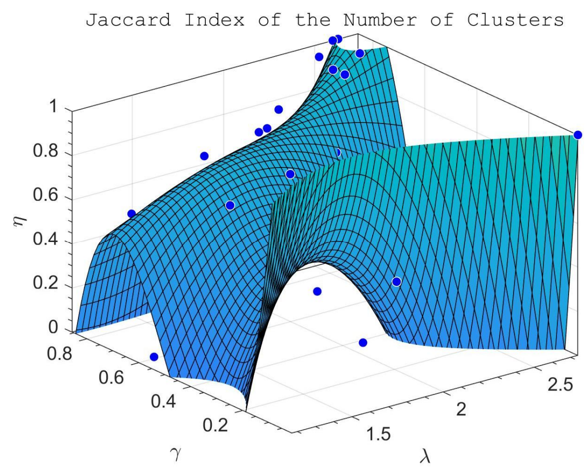

Figure 8: Jaccard index of the number clusters vs λ and γ for Indoor B2

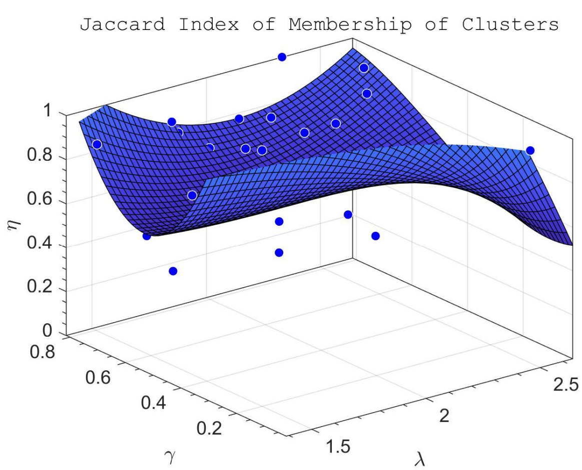

Figure 7: Jaccard index of membership of clusters vs λ and γ for Indoor B1

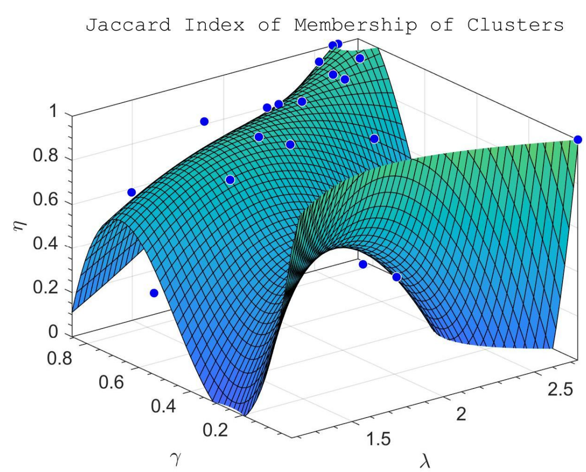

Figure 9: Jaccard index of membership of clusters vs λ and γ for Indoor B2

$$\eta = \frac{|C_{\text{ref}} \cap C_{\text{calc}}|}{|C_{\text{ref}} \cup C_{\text{calc}}|} = \frac{M_{11}}{M_{11} + M_{10} + M_{01}} \quad \in [0,1] \tag{6}$$

multipath clustering are the following:

1. Indoor, B1, line-of-sight, single link
2. Indoor, B2, line-of-sight, single link

where $|\cdot|$ refers to cardinality, M_{11} is the total number of multipath clusters for the accuracy on the number clusters or total number of multipaths for the accuracy on the membership of the clusters in C_{ref} that are the same as in C_{calc}, M_{10} is the total number of multipath clusters for the accuracy on the number of clusters or total number of multipaths for the accuracy on the membership of the clusters in C_{ref} that are not in C_{calc}, and M_{01} is the total number of multipath clusters for the accuracy on the number clusters or total number of multipaths for the accuracy on the membership of the clusters in C_{calc} that are not in C_{ref}.

SCAMS gives the correct number of clusters by using the calculated value of $\lambda > 0$ from [13] and choosing the correct value of γ in the range (0, 1). Using a value of γ that is less than the correct value leads to a lesser number of clusters than the correct number of clusters while a higher value of γ results to a higher number of clusters than the correct number of clusters. An incorrect combination of λ and γ tend to give the trivial solution. Figure 2a shows the Jaccard index of the clusters in Indoor B1 versus the corresponding values of λ and γ. The minimum index is 0.1176 while the maximum index is 1. Figure 2b presents the Jaccard index of the members per cluster in Indoor B1. The minimum index is 0.3649 while the maximum index is 1. Figure 3a demonstrates the Jaccard index of the clusters in Indoor B2. The minimum index is 0 while the maximum index is 1. Figure 3b illustrates the Jaccard index of the members per cluster of Indoor B2. The minimum index is 0.3684 while the maximum index is 1. Indoor B1 has 50% of the indices above the mean (red dots) for the number of clusters while 47% for the membership of the clusters. Indoor B2 has 57% of the indices above the mean (red dots) for the number of clusters while 53% for the membership of the clusters. SCAMS exhibits promising results and gives higher accuracy compared to the results obtained in [1].

The relative frequency of the Jaccard indices on the number of clusters and the membership of the clusters for Indoor B1 is shown in Figure 4. For the number of clusters, 23% of the indices occurred at 0.6 and 0.7 while 72% are indices at least 0.6. For the membership of the clusters, 30 % of the indices occurred at 0.8 while 77% are indices at least 0.7. Figure 5 shows the relative frequency of the Jaccard indices for Indoor B2. For the number of clusters, 27% of the indices is 1 while half of the indices are at least 0.7. For the membership of the clusters, 37% of the indices is 1 while 67% of the indices is at least 0.8. SCAMS registered an index of 1 for both Indoor B1 and Indoor B2 with a mean of 25.5%. A Jaccard index of 1 means that the multipaths are clustered accurately.

Figure 6 displays a surface fit of the Jaccard index of the number of clusters of Indoor B1 as a function of λ and γ. The mathematical model generated is

$$\begin{aligned}\eta = {} & 6.257 - 1.168\lambda - 19.49\gamma - 0.3914\lambda^2 \\ & +2.898\lambda\gamma + 22.51\gamma^2 + 1.548\lambda^2\gamma \\ & -7.177\lambda\gamma^2 - 1.755\gamma^3\end{aligned} \quad . \qquad (7)$$

For the membership of clusters for Indoor B1, the surface fit is shown in Figure 7. The mathematical model generated is

$$\begin{aligned}\eta = {} & 3.092 + 0.7946\lambda - 12.53\gamma - 0.6683\lambda^2 \\ & +0.1517\lambda\gamma + 18.13\gamma^2 + 1.662\lambda^2\gamma \\ & -5.792\lambda\gamma^2 - 1.881\gamma^3\end{aligned} \quad . \qquad (8)$$

Figure 8 illustrates the surface fit for the number of clusters for Indoor B2. The mathematical model generated is

$$\begin{aligned}\eta = {} & -9.901 + 15.44\lambda - 1.683\gamma - 4.157\lambda^2 \\ & - 23.34\lambda\gamma + 44.88\gamma^2 + 5.635\lambda^2\gamma \\ & +3.807\lambda\gamma^2 - 32.72\gamma^3\end{aligned} \quad . \qquad (9)$$

For the membership of clusters for Indoor B2, Figure 9 presents the surface fit. The mathematical model generated is

$$\begin{aligned}\eta = {} & -6.148 + 8.602\lambda + 2.98\gamma - 2.173\lambda^2 \\ & - 13.33\lambda\gamma + 19.9\gamma^2 + 2.661\lambda^2\gamma \\ & +4.131\lambda\gamma^2 - 17.97\gamma^3\end{aligned} \quad . \qquad (10)$$

The coefficients of (7)–(10) have 95% confidence bounds. The value of the Jaccard index can be determined using the mathematical model by specifying first the values of λ and γ.

5. CONCLUSION

This paper presents for the first time the results of SCAMS when applied to cluster multipaths. SCAMS determines simultaneously the number of clusters and the membership of the clusters which are dependent on the values of λ and γ. C2CM Indoor B1 and Indoor B2 LOS single link from the IEEE DataPort were used as reference data. The whitened data were first normalized to make the values of the affinities positive and to give better clustering results. Results show that SCAMS gives better clustering accuracy than the approaches in [1]. Thus, SCAMS can be used as an alternative clustering approach in COST 2100 channel modeling.

ACKNOWLEDGEMENT

The authors would like to thank the Department of Science and Technology-Engineering Research and Development for Technology (DOST-ERDT) for the financial support and Dr. Zhuwen Li for insights on SCAMS.

REFERENCES

1. D. Abinoja and L. Materum. **Evaluation of techniques for identifying multipath propagation clusters in wireless systems by Bayesian information criterion model-based clustering**, accepted for publication.
2. J. Blanza, A. Teologo, and L. Materum. **Datasets for multipath clustering at 285 MHz and 5.3 GHz bands based on COST 2100 MIMO channel model**, [Online]. Available: http://dx.doi.org/10.21227/4cb9-hf81, 2019.

3. J. Blanza, A. Teologo, and L. Materum. **Datasets for multipath clustering at 285 MHz and 5.3 GHz bands based on COST 2100 MIMO channel model**, accepted in *9th Int. Symp. Multimedia Commun.*, 2019.
4. Z. Li, L. Cheong, and S. Zhou. **SCAMS: Simultaneous clustering and model selection**, in *Proc. IEEE Conf. Comput. Vision Pattern Recognit.*, 2014, pp 264-271.
5. S. Ibrahim, M. Rozan, and N. Sabri. **Comparative Analysis of Support Vector Machine (SVM) and Convolutional Neural Network (CNN) for White Blood Cells' Classification**, *Int. J. Adv. Trends Comput. Sci. Eng.*, vol. 8, no. 1.3, pp. 394-399, 2019. https://doi.org/10.30534/ijatcse/2019/6981.32019
6. B. Chandirika, N.K. Sakthivel, and S. Subasree. **An Energy Efficient K-Means Clustering based Trust Model for Wireless Sensor Networks**, *Int. J. Adv. Trends Comput. Sci. Eng.*, vol. 8, no. 2, pp. 144-153, 2019. https://doi.org/10.30534/ijatcse/2019/08822019
7. N. Czink, P. Cera, J. Salo, E. Bonek, J. Nuutinen, and J. Ylitalo. **A framework for automatic clustering of parametric MIMO channel data including path powers**, in *IEEE 64th Veh. Technol. Conf.*, 2006, pp. 1-5. https://doi.org/10.1109/VTCF.2006.35
8. C. Gentile. **Using the kurtosis measure to identify clusters in wireless channel impulse responses**, *IEEE Trans. Antennas Propag.*, vol. 61, no. 6, pp. 3392-3395, 2013. https://doi.org/10.1109/TAP.2013.2253299
9. R. He, Q. Li, B. Ai, Y. Geng, A. Molisch, V. Kristem, Z. Zhong, and J. Yu. **A kernel-power-density-based algorithm for channel multipath components clustering**, *IEEE Trans. Wireless Commun.*, vol. 16, no. 11, pp. 7138-7151, 2017. https://doi.org/10.1109/TWC.2017.2740206
10. Y. Li, J. Zhang, Z. Ma, and Y. Zhang. **Clustering analysis in the wireless propagation channel with a variational Gaussian mixture model**, *IEEE Trans. Big Data*, 2018.
11. L. Liu, C. Oestges, J. Poutanen, K. Haneda, P. Vainikainen, F. Quitin, F. Tufvesson, and P. De Doncker. **The COST 2100 MIMO channel**, *IEEE Trans. Wireless Commun.*, vol. 19, no. 6, pp. 92-99, 2012. https://doi.org/10.1109/MWC.2012.6393523
12. R. Verdone and A. Zanella. **Pervasive Mobile and Ambient Wireless Communications: COST Action 2100**, Springer Science & Business Media, 2012, ch. 3. https://doi.org/10.1007/978-1-4471-2315-6
13. E. Elhamifar and R. Vidal. **Sparse subspace clustering: Algorithm, theory, and applications**, *IEEE Trans Pattern Anal. Mach. Intell.*, vol. 35, np. 11, pp. 2765-2781, 2013. https://doi.org/10.1109/TPAMI.2013.57
14. S. Boyd, N. Parikh, E. Chu, B. Peleato, J. Eckstein, et al. **Distributed optimization and statistical learning via the alternating direction method of multipliers**, *Found. Trends Mach. Learn.*, vol. 3, no. 1, pp. 1-122, 2011 https://doi.org/10.1561/2200000016